

# Theoretical study of the photoelectron spectrum of ethyl formate: Ab initio and density functional theory investigation

Marta Łabuda<sup>1,a</sup> and Julien Guthmuller<sup>1,b</sup>

<sup>1</sup>Department of Theoretical Physics and Quantum Information, Faculty of Applied Physics and Mathematics, Gdańsk University of Technology, Narutowicza 11/12, 80-233 Gdańsk, Poland

**Abstract.** The first ionization energy and associated photoelectron spectrum of ethyl formate are investigated with quantum chemistry calculations. The geometries, harmonic vibrational frequencies and first ionization energy are computed at the Hartree-Fock (HF) and at the second order Møller-Plesset perturbation theory (MP2). Moreover, accurate ionization energies are obtained with the Coupled-Cluster theory including singles and doubles excitations (CCSD) as well as singles, doubles and perturbative triples excitations (CCSD(T)). Then, these *ab initio* results are assessed with respect to experimental values. Additionally, the ionization energies are also calculated with the computationally attractive density functional theory (DFT). In this case the accuracy of several exchange-correlation functionals is evaluated by comparison with the *ab initio* and experimental results. In a next step, the vibrational structure of the photoelectron spectrum is simulated at the HF, MP2 and DFT levels via the calculation of the Franck-Condon factors. These simulations are compared to the experimental photoelectron spectrum and allow an accurate reproduction of the vibrational progression.

## 1 Introduction

The calculation of accurate ionization energies and the simulation of photoelectron vibrational structure are of great importance for the interpretation of experimental results and consequently for the understanding of molecular functions (see e.g. [1][2][3][4][5]). For example, the ionization energies and vibrational structure of the photoelectron spectra of methyl formate [1] and limonene [2] were recently investigated by combining experimental results with *ab initio* calculations. These studies have provided a reliable assignment of the electronic and vibrational bands of the investigated compounds.

An important issue in this field is the determination of accurate theoretical values for the first ionization energies. This can usually be obtained using high level coupled-cluster methods in association with large basis sets. However, due to the significant

---

<sup>a</sup> e-mail: [marta@mif.pg.gda.pl](mailto:marta@mif.pg.gda.pl)

<sup>b</sup> e-mail: [jguthmuller@mif.pg.gda.pl](mailto:jguthmuller@mif.pg.gda.pl)

computational cost of such calculations, especially for large molecules, it is of interest to investigate the accuracy of methods based on the density functional theory, which are computationally less demanding. In this respect, newly developed long range corrected functionals and double hybrid functionals present interesting features for the calculation of ionization energies. Additionally, density functional theory methods are also attractive for the fast calculation of the Franck-Condon vibrational structure of photoelectron spectra. Therefore, it is of interest to evaluate how accurately such methods can describe ionization energies as well as vibrational structures, and how they compare to *ab initio* calculations.

In this purpose, the present contribution focuses on the calculation of the first ionization energy and vibrational structure of the photoelectron spectrum for the most stable conformer of ethyl formate [6][7]. Ethyl formate represents a medium sized model compound, which allows the assessment of several theoretical methods. Moreover, theoretical calculations will also be compared with new experimental results obtained in the gas phase [8]. The paper is organized as follows: Section 2 describes the computational and theoretical methods, Section 3 presents the results and discussions concerning the geometries (3.1), ionization energies (3.2) and photoelectron vibrational structures (3.3) of ethyl formate, while conclusions are given in Section 4.

## 2 Computational and theoretical methods

The ground state geometry, harmonic vibrational frequencies, and normal coordinates of the neutral singlet state ( $S_0$ ) and ionic doublet state ( $D_0$ ) of ethyl formate were obtained with the GAUSSIAN 09 program [9] by means of density functional theory (DFT), Hartree-Fock (HF) and second-order Møller-Plesset (MP2) calculations. The ionic state was described by open-shell unrestricted calculations. The DFT calculations were performed with the B3LYP [10][11],  $\omega$ B97X [12], LC-BLYP [13][11][14] and B2PLYP-D [15] exchange-correlation (XC) functionals in association with the aug-cc-pVTZ basis set [16]. B3LYP is a hybrid functional containing 20% of HF exchange,  $\omega$ B97X and LC-BLYP belong to the family of long range corrected functionals and B2PLYP-D is a double hybrid functional containing 53% of HF exchange, MP2-like correlation and dispersion corrections. The first ionization energies (IE) were computed from the energy difference between the neutral and ionic ground states. The vertical IE was calculated at the ground state geometry of the neutral compound and the adiabatic IE was evaluated using the optimized geometries of the neutral and ionic ground states. The zero point vibrational energy (ZPVE) correction to the adiabatic energy was determined from the harmonic vibrational frequencies. Additionally, the first ionization energies were calculated with the coupled-cluster singles and doubles (CCSD), and the coupled-cluster singles, doubles and perturbative triples (CCSD(T)) methods, employing the optimized geometries at the MP2/aug-cc-pVTZ level of approximation. In order to investigate the basis set convergence, MP2, CCSD and CCSD(T) energy calculations were performed both with the aug-cc-pVTZ and aug-cc-pVQZ basis sets.

The simulation of the vibrational structure of the first photoelectron band requires the determination of the multidimensional Franck-Condon (FC) factors. According to Duschinsky [17], the harmonic vibrational normal coordinates  $Q'$  of the initial state ( $S_0$  state) can be related to the normal coordinates of the final state ( $D_0$  state) according to the relation,

$$Q' = JQ + K \quad (1)$$

in which  $K$  is the displacement vector, representing the difference of geometry between the two states, and  $J$  is the Duschinsky rotation matrix, describing the changes

in the normal coordinates. Within the harmonic approximation, the FC factors can be calculated using recursive relations [18][19]. These relations were implemented in a program developed by one of the author [20][21], which makes use of the ground state geometries, harmonic frequencies and normal coordinates calculated for the neutral ( $S_0$  state) and ionic ( $D_0$  state) forms. In order to investigate the impact of including Duschinsky rotation effects, the FC factors were also calculated within the independent mode displaced harmonic oscillator model (IMDHOM). This approximation takes into account the geometrical differences between the initial and final states but neglects modifications of the vibrational frequencies and Duschinsky rotation effects (i.e.  $J=1$  in equation (1)). Finally, to simulate the experimental broadening of the photoelectron spectrum the vibronic transitions were broadened by a Gaussian function with a full width at half maximum set to  $400\text{ cm}^{-1}$ .

### 3 Results and discussion

#### 3.1 Geometries of ethyl formate

The geometries of the most stable conformer [7] (s-cis,trans) of ethyl formate (see Figure 1) were calculated at the HF, MP2, B3LYP, B2PLYP-D,  $\omega$ B97X and LC-BLYP levels of approximations employing the aug-cc-pVTZ basis set. The bond lengths, bond angles and dihedral angles of the neutral ( $S_0$  state) and ionic ( $D_0$  state) structures are reported in Tables 1-3.

**Table 1.** Calculated geometries (HF and MP2) of ethyl formate (s-cis,trans) using the aug-cc-pVTZ basis set

	HF			MP2		
	$S_0$	$D_0$	$D_0-S_0$	$S_0$	$D_0$	$D_0-S_0$
Bond lengths (Å)						
O5-C2	1.179	1.268	0.089	1.208	1.275	0.067
C2-O1	1.311	1.222	-0.089	1.340	1.252	-0.088
O1-C3	1.425	1.522	0.097	1.447	1.529	0.082
C3-C4	1.510	1.501	-0.009	1.508	1.495	-0.013
C2-H6	1.085	1.083	-0.002	1.094	1.095	0.001
C3-H7	1.081	1.078	-0.003	1.089	1.088	-0.001
C3-H8	1.081	1.078	-0.003	1.089	1.088	-0.001
C4-H9	1.083	1.083	0.000	1.089	1.090	0.001
C4-H10	1.083	1.080	-0.003	1.088	1.087	-0.001
C4-H11	1.083	1.080	-0.003	1.088	1.087	-0.001
Bond angles (°)						
O5-C2-O1	125.9	124.1	-1.8	125.8	124.8	-1.0
C2-O1-C3	117.8	123.5	5.7	114.5	118.5	4.0
O1-C3-C4	107.8	106.5	-1.3	107.0	106.2	-0.8
O5-C2-H6	123.8	115.1	-8.7	125.0	114.8	-10.2
O1-C3-H7	108.8	105.0	-3.8	108.5	104.8	-3.7
C3-C4-H9	109.6	107.5	-2.1	109.6	107.5	-2.1
Dihedral angles (°)						
O5-C2-O1-C3	0.0	0.0	0.0	0.0	0.0	0.0
C2-O1-C3-C4	180.0	180.0	0.0	180.0	180.0	0.0
O1-C3-C4-H9	180.0	180.0	0.0	180.0	180.0	0.0



**Table 2.** Calculated geometries (B3LYP and B2PLYP-D) of ethyl formate (s-cis,trans) using the aug-cc-pVTZ basis set

	B3LYP			B2PLYP-D		
	$S_0$	$D_0$	$D_0-S_0$	$S_0$	$D_0$	$D_0-S_0$
Bond lengths (Å)						
O5-C2	1.201	1.260	0.059	1.204	1.267	0.063
C2-O1	1.337	1.252	-0.085	1.338	1.254	-0.084
O1-C3	1.452	1.542	0.090	1.451	1.545	0.094
C3-C4	1.511	1.492	-0.019	1.509	1.495	-0.014
C2-H6	1.097	1.105	0.008	1.095	1.100	0.005
C3-H7	1.090	1.094	0.004	1.089	1.088	-0.001
C3-H8	1.090	1.087	-0.003	1.089	1.088	-0.001
C4-H9	1.090	1.093	0.003	1.090	1.091	0.001
C4-H10	1.090	1.088	-0.002	1.089	1.087	-0.002
C4-H11	1.090	1.091	0.001	1.089	1.087	-0.002
Bond angles (°)						
O5-C2-O1	126.1	126.8	0.7	125.9	125.7	-0.2
C2-O1-C3	116.5	119.0	2.5	115.5	119.2	3.7
O1-C3-C4	107.8	107.3	-0.5	107.3	106.3	-1.0
O5-C2-H6	124.7	113.9	-10.8	124.8	114.3	-10.5
O1-C3-H7	108.4	105.2	-3.2	108.4	104.4	-4.0
C3-C4-H9	109.6	107.7	-1.9	109.5	107.4	-2.1
Dihedral angles (°)						
O5-C2-O1-C3	0.0	-1.4	-1.4	0.0	0.0	0.0
C2-O1-C3-C4	180.0	149.8	-30.2	180.0	180.0	0.0
O1-C3-C4-H9	180.0	177.0	-3.0	180.0	180.0	0.0

**Table 3.** Calculated geometries ( $\omega$ B97X and LC-BLYP) of ethyl formate (s-cis,trans) using the aug-cc-pVTZ basis set

	$\omega$ B97X			LC-BLYP		
	$S_0$	$D_0$	$D_0-S_0$	$S_0$	$D_0$	$D_0-S_0$
Bond lengths (Å)						
O5-C2	1.198	1.262	0.064	1.191	1.254	0.063
C2-O1	1.331	1.247	-0.084	1.320	1.238	-0.082
O1-C3	1.441	1.525	0.084	1.428	1.501	0.073
C3-C4	1.508	1.495	-0.013	1.496	1.485	-0.011
C2-H6	1.097	1.101	0.004	1.096	1.103	0.007
C3-H7	1.090	1.090	0.000	1.089	1.089	0.000
C3-H8	1.090	1.090	0.000	1.089	1.089	0.000
C4-H9	1.090	1.091	0.001	1.088	1.089	0.001
C4-H10	1.089	1.088	-0.001	1.087	1.087	0.000
C4-H11	1.089	1.088	-0.001	1.087	1.087	0.000
Bond angles (°)						
O5-C2-O1	125.7	125.6	-0.1	125.2	125.3	0.1
C2-O1-C3	115.9	119.3	3.4	116.2	119.9	3.7
O1-C3-C4	107.6	106.9	-0.7	107.8	107.2	-0.6
O5-C2-H6	124.6	114.3	-10.3	124.5	114.1	-10.4
O1-C3-H7	108.5	104.9	-3.6	108.5	105.3	-3.2
C3-C4-H9	109.7	107.7	-2.0	109.9	108.1	-1.8
Dihedral angles (°)						
O5-C2-O1-C3	0.0	0.0	0.0	0.0	0.0	0.0
C2-O1-C3-C4	180.0	180.0	0.0	180.0	180.0	0.0
O1-C3-C4-H9	180.0	180.0	0.0	180.0	180.0	0.0

All calculated geometries correspond to stable structures because no imaginary frequencies were obtained in the harmonic frequencies calculations. It is seen from the Table 1 that the HF method mostly predicts shorter bond lengths than the MP2 calculations. Similarly, the LC-BLYP functional gives shorter bond lengths in comparison to the other functionals (Tables 2 and 3) and to the MP2 method. More importantly, it is found that the main geometrical changes ( $D_0-S_0$ ) going from the  $S_0$  state to the  $D_0$  state occur for the three bonds O5-C2, C2-O1 and O1-C3 as well as for the angle O5-C2-H6. Additionally, it is seen that the HF method provides the largest bond length changes, whereas the LC-BLYP functional gives bond length changes of about 0.005 to 0.025 Å smaller. The MP2 method and the other XC functionals present bond length changes comprised between the HF and the LC-BLYP values with the exception of the O5-C2 bond obtained with B3LYP. The changes in the angle O5-C2-H6 are very similar between the MP2 and DFT methods with values comprised between -10.2 and -10.8°, whereas the HF method gives a smaller value of -8.7°. It can also be mentioned that the bond length C3-C4 and the angles C2-O1-C3 and O1-C3-H7 show non negligible variations. Moreover, as it can be seen from the values of the dihedral angles, almost all geometries possess a plane of symmetry i.e. belong to the  $C_s$  point group. The only exception concerns the geometry of the  $D_0$  state obtained with the B3LYP functional, which presents a significant rotation of about -30° along the O1-C3 bond going from the  $S_0$  state to the  $D_0$  state. The fact that the symmetry of the ionic state is only broken using the B3LYP method is an indication that this functional might be unsuitable to describe the open-shell electronic structure of the  $D_0$  state.

### 3.2 First ionization energies of ethyl formate

The calculated vertical and adiabatic first ionization energies of ethyl formate are reported in Table 4. The experimental values in gas phase are also given for comparison. The vertical ionization energy obtained at the HF level is significantly underestimated by 1.321 eV in comparison to the experimental estimation. On the contrary, the values calculated with the MP2 method present overestimations of 0.556 and 0.625 eV with the aug-cc-pVTZ and aug-cc-pVQZ basis sets, respectively. Significant improvements are obtained with the CCSD and CCSD(T) methods, which show deviations of 0.076 and 0.156 eV, respectively, using the aug-cc-pVTZ basis set. Nevertheless, calculations performed employing the larger aug-cc-pVQZ basis set do not improve further the agreement with the experimental vertical IE and show deviations of 0.132 and 0.217 eV with CCSD and CCSD(T), respectively. In principle, the high level CCSD(T)/aug-cc-pVQZ method should provide the best estimation of the IE and consequently the calculated value of 10.988 eV can be considered as a reference for the vertical IE. Therefore, the fact that the CCSD method gives vertical IE in better agreement with experiment than CCSD(T) results, and the fact that calculations performed with the aug-cc-pVTZ basis set are closer to experiment than those obtained with the aug-cc-pVQZ basis set, are an indication that the comparison with experiment is not totally adequate. Indeed, the calculated vertical IE does not take into account the vibrational structure of the first photoelectron band (see next section), while the experimental value of 10.771 eV is associated to the most intense vibrational band of the measured photoelectron spectrum (Figure 1). This illustrates the limits of comparing experimental estimations of the vertical IE with calculations neglecting the vibrational structure of the photoelectron spectrum. The vertical IE obtained with the DFT methods B3LYP,  $\omega$ B97X and B2PLYP-D are underestimated with respect to the CCSD(T)/aug-cc-pVQZ reference value by 0.217, 0.156 and 0.112 eV, whereas the LC-BLYP vertical IE provides the best agreement with an overestimation of only

0.091 eV. These differences in IE can be related to the different treatments of the HF exchange in the functionals i.e. functionals including a larger amount of HF exchange tend to give larger IE.

**Table 4.** Vertical and adiabatic first ionization energies (eV) of ethyl formate (s-cis,trans) using the aug-cc-pVTZ basis set

Method	Vertical <sup>c</sup>	Adiabatic <sup>c</sup>	ZPVE correction	Adiabatic+ZPVE <sup>c</sup>
HF	9.450	8.893	-0.044	8.849
MP2	11.327 (11.396)	10.929 (11.001)	-0.039	10.890 (10.962)
CCSD <sup>a</sup>	10.847 (10.903)	10.471 (10.530)	-0.039 <sup>b</sup>	10.432 (10.491)
CCSD(T) <sup>a</sup>	10.927 (10.988)	10.579 (10.644)	-0.039 <sup>b</sup>	10.540 (10.605)
B3LYP	10.771	10.461	-0.079	10.382
$\omega$ B97X	10.832	10.473	-0.057	10.416
B2PLYP-D	10.876	10.532	-0.059	10.473
LC-BLYP	11.079	10.721	-0.061	10.660
Experiment <sup>d</sup>	10.771	10.588	—	10.588

<sup>a</sup> Calculated with the MP2/aug-cc-pVTZ geometry

<sup>b</sup> ZPVE correction (-0.039 eV) calculated at the MP2/aug-cc-pVTZ level

<sup>c</sup> Values in brackets are calculated with the aug-cc-pVQZ basis set using the MP2/aug-cc-pVTZ geometry

<sup>d</sup> Measured values in gas phase [8]

The calculated adiabatic IEs (Table 4) show similar trends as the vertical IEs going from one theoretical method to the other. Indeed, the HF value is significantly underestimated in comparison to the experimental adiabatic value of 10.588 eV, while the MP2 method overestimates the adiabatic IE by 0.341 and 0.413 eV with the aug-cc-pVTZ and aug-cc-pVQZ basis sets, respectively. However, the calculated IEs at the CCSD(T) level are much closer to the experimental result with an overestimation of only 0.056 eV using the larger aug-cc-pVQZ basis set. The adiabatic IEs obtained at the DFT level with the functionals B3LYP,  $\omega$ B97X and B2PLYP-D are underestimated both in comparison to experiment and to the CCSD(T)/aug-cc-pVQZ reference value, whereas, similarly to the vertical IE, the LC-BLYP functional overestimates the adiabatic IE. By taking into account the vibrational energy described by the ZPVE correction, it is found that the best agreement with the experimental value is obtained for the CCSD(T)/aug-cc-pVQZ method with an overestimation of only 0.017 eV. Therefore, this demonstrates that a reliable comparison with experimental results can be performed using calculated adiabatic IE including vibrational corrections. The deviations obtained at the DFT levels are comprised between -0.206 and 0.072 eV, while the best results are obtained for the double hybrid functional B2PLYP-D and the long range corrected functional LC-BLYP with deviations of -0.115 and 0.072 eV, respectively. It can also be mentioned that the calculated B3LYP IE has still a reasonable value despite the fact that the  $D_0$  state has a much different geometry than those obtained with the other theoretical methods. This indicates that the geometry does not have a strong effect on the value of the IE. Even if slightly less accurate than CCSD(T) calculations, the results obtained by the DFT methods are of interest because such calculations are much less computationally expensive than high level coupled-cluster calculations.

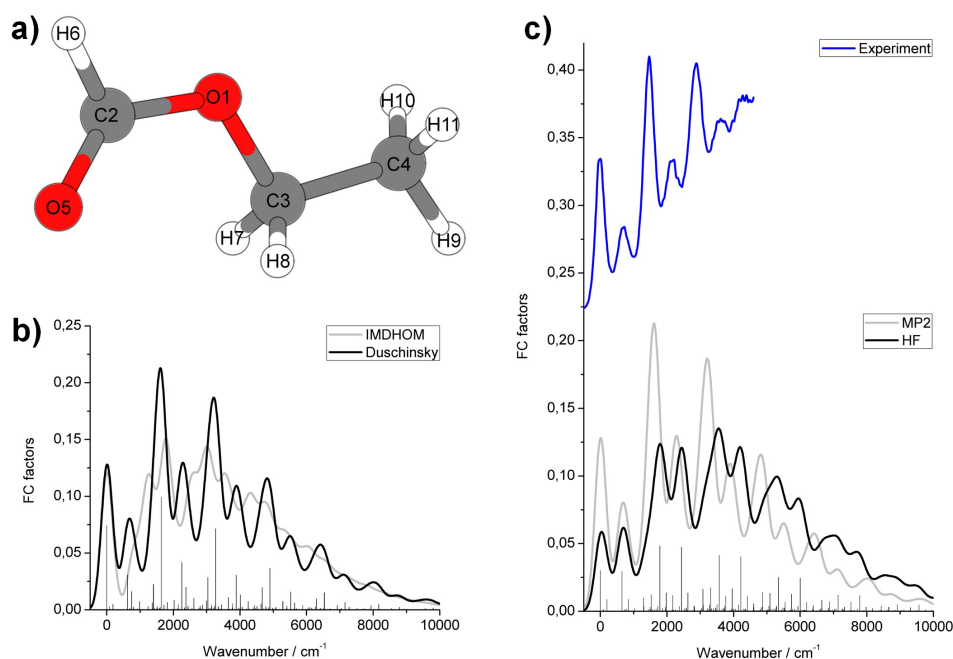


**Fig. 1.** a) Structure of ethyl formate (s-cis,trans) and atomic numbering, b) Comparison between the FC vibrational structures of the first photoelectron band calculated at the MP2 level within the IMDHOM and including Duschinsky rotation effects, c) Comparison between the experimental first photoelectron band [8] and the calculated FC vibrational structures obtained at the HF and MP2 levels of approximation.

In summary, it is found that: (i) the calculated IE (adiabatic + ZPVE) at the CCSD(T)/aug-cc-pVQZ level is in excellent agreement with experiment and consequently can be considered as a reference value, (ii) the DFT results obtained with the B2PLYP-D and LC-BLYP functionals have comparable accuracies as the CCSD/aug-cc-pVQZ method, which shows a deviation with respect to experiment of -0.097 eV, (iii) the IEs calculated at the MP2 level are less accurate as DFT IEs and are noticeably overestimated in comparison to experiment, and (iv) the IEs obtained at the HF level are strongly underestimated and inaccurate.

### 3.3 Vibrational structure of the first photoelectron band of ethyl formate

The vibrational structure of the first photoelectron band of ethyl formate was simulated from the FC factors, which were calculated between the neutral state  $S_0$  and the ionic state  $D_0$ . The discussion of the vibrational structure is limited to calculations performed with the MP2 and DFT methods. Coupled-cluster calculations were not carried out because they have a prohibitive computational cost, which prevent their use for the determination of the geometries and harmonic vibrational frequencies.

The vibrational structure at the MP2 level was simulated by employing the IMDHOM and by including Duschinsky rotation effects. The use of the IMDHOM is motivated by the fact that this approximation was found to give a realistic description of the absorption spectra of several chromophores (see e.g. [20][21]) and of associated properties like e.g. resonance Raman intensities (see e.g. [22][23]). However, in

the case of the photoelectron spectrum of ethyl formate, it is seen on Figure 1 that significant differences are obtained between both approaches. This demonstrates that the inclusion of Duschinsky rotation effects is mandatory in order to describe the vibrational structure of the ethyl formate photoelectron spectrum. This conclusion is also confirmed by comparison with the experimental spectrum reported on Figure 1, and shows that the IMDHOM is inappropriate to describe the vibrational structure of the photoelectron spectrum. Therefore, in the following only the spectra calculated by including Duschinsky rotation effects are presented.

The photoelectron spectrum simulated at the MP2 level shows a good agreement with the experimental spectrum (Figure 1). Indeed, the main vibrational bands and their relative intensities are correctly reproduced by the calculations. However, the spectrum obtained at the HF level presents a less good agreement with respect to experiment, displaying inaccurate relative intensities as e.g. between the adiabatic band 0-0 and the band at about  $600\text{ cm}^{-1}$ . These disagreements can be related to the large bond length changes obtained at the HF level going from the  $S_0$  state to the  $D_0$  state (see Table 1). Additionally, this explains the fact that the 0-0 FC factor is much smaller at the HF level than the one obtained with MP2. The inaccuracy of the HF geometries and related FC factors was expected, since this method neglects the correlation energy.

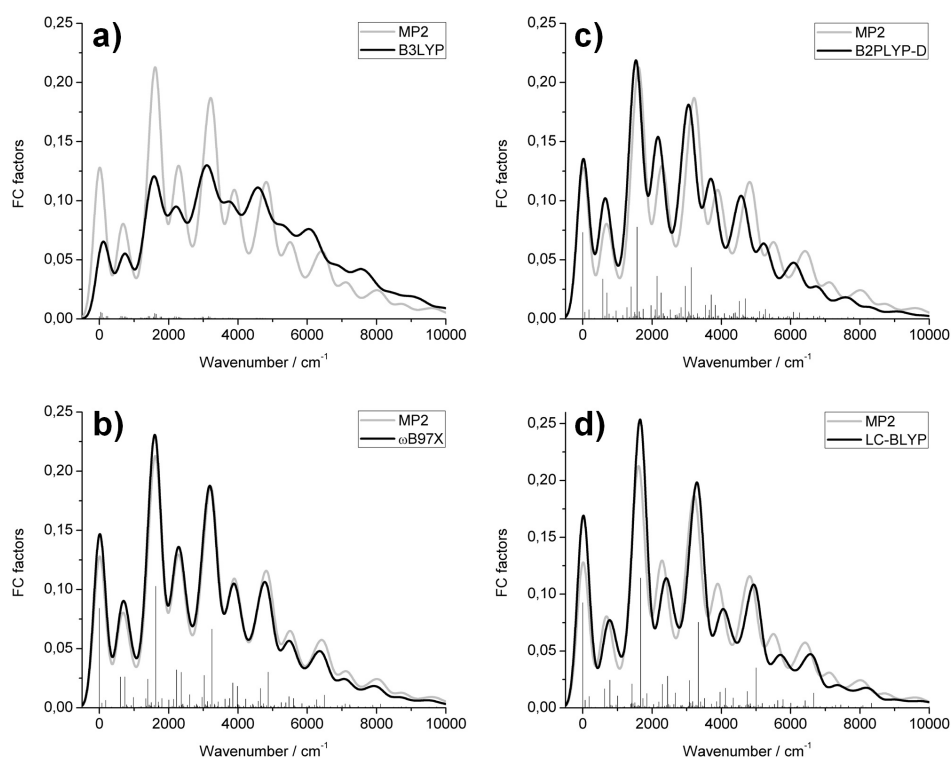


**Fig. 2.** Comparison between the calculated FC vibrational structures obtained at the MP2 level of approximation with the a) B3LYP, b)  $\omega$ B97X, c) B2PLYP-D and d) LC-BLYP theoretical spectra.



Next, the MP2 spectrum is compared to the spectra simulated with the B3LYP,  $\omega$ B97X, B2PLYP-D and LC-BLYP functionals (see Figure 2) in order to assess the quality of the DFT calculations. Similarly to the HF results, the spectrum simulated with the B3LYP functional displays inaccurate relative intensities in comparison to the experimental and MP2 spectra. This concerns the relative intensities between the two first bands (0-0 and at about  $600\text{ cm}^{-1}$ ) as well as between the successive pairs of bands e.g. at about  $1600$  and  $2200\text{ cm}^{-1}$  and at about  $3300$  and  $3900\text{ cm}^{-1}$ . The B3LYP vibrational progression can be related to the large rotation occurring along the O1-C3 bond going from the  $S_0$  state to the  $D_0$  state, which also explains the too small intensity of the adiabatic band obtained with this functional. This confirms that the geometry of the ionic state obtained with the B3LYP functional is not reliable. However, the spectrum calculated with the long range corrected functional  $\omega$ B97X is very close to the MP2 spectrum as could be expected by investigating their almost similar geometrical changes obtained between the neutral and ionic states (Tables 1 and 3). The only differences concern a slightly more pronounced adiabatic band for the  $\omega$ B97X spectrum and some minor changes in the vibrational progression. Consequently, both the MP2 and  $\omega$ B97X spectra present a similar agreement with the experimental spectrum. Next, the B2PLYP-D spectrum shows more important differences with the MP2 spectrum than the  $\omega$ B97X results. In particular, the relative intensities of the bands at about  $600$  and  $2200\text{ cm}^{-1}$  are larger in comparison to MP2, which worsen the agreement with the experimental spectrum. Finally, an opposite behavior is found for the LC-BLYP functional, which displays weaker relative intensities for the bands at about  $600$  and  $2200\text{ cm}^{-1}$  as well as a more intense adiabatic band. This effect can be related to the rather smaller geometrical changes in the bond lengths obtained with this functional between the neutral and ionic states as e.g. for the bond O1-C3 (Table 3). Overall, these differences appear to improve the agreement with the experimental spectrum. Additional differences between the methods concern the position of the vibrational bands. It is well known that vibrational frequencies obtained within the harmonic approximation present deviations with respect to experimental results [24], which can be corrected by the use of scale factors. However, for a matter of comparison between the methods, scale factors were not employed in the present study. Thus, it is seen that the HF and LC-BLYP methods tend to overestimate the vibrational frequencies in comparison to the MP2 or  $\omega$ B97X approaches. In summary, it is found that: (i) the IMDHOM is not adequate to simulate the vibrational structure of the photoelectron spectrum and that Duschinsky rotation effects must be included, (ii) the HF and B3LYP methods provide inaccurate photoelectron spectra due to overestimated geometrical changes obtained between the  $S_0$  and  $D_0$  states, and (iii) the spectra simulated with the MP2,  $\omega$ B97X and LC-BLYP methods present a good agreement with the experimental spectrum and consequently, these methods are suitable to describe the vibrational structure of the photoelectron spectrum.

## 4 Conclusions

The geometries, first ionization energies and vibrational structures of the first photoelectron band of ethyl formate were calculated with the HF, MP2 and CCSD(T) *ab initio* methods as well as with DFT based approaches. The comparison between theoretical and experimental results has shown that the adiabatic IE including ZPVE corrections calculated at the CCSD(T)/aug-cc-pVQZ level is in excellent agreement with the experimental result and can be considered as a reference value. The IEs obtained with the B2PLYP-D and LC-BLYP functionals have comparable accuracies as the CCSD/aug-cc-pVQZ method, whereas the MP2 and HF approaches are less

accurate. The investigation of the photoelectron spectra has shown that Duschinsky rotation effects are mandatory to describe the vibrational structure. Additionally, the MP2,  $\omega$ B97X and LC-BLYP methods are found to provide spectra in equal agreement with the experimental spectrum, whereas the HF and B3LYP methods are less accurate due to incorrect geometries. Finally, it can be concluded that the LC-BLYP functional provides the most balanced description of both the IEs and the photoelectron vibrational structure associated to the attractive computational cost of DFT calculations.

**Acknowledgements** The authors are thankful to Dr. Vincent Liégeois for fruitful discussions about the calculation of FC factors and to Dr. Małgorzata Śmiałek-Telega for providing experimental data. The authors are also thankful to the 7<sup>th</sup> Framework Programme of the European Union for their respective Marie Curie Re-Integration Grant (DYNAMICOL) and Marie Curie Career Integration Grant (VIBRAMAN). The calculations have been performed at the Academic Computer Center (TASK) in Gdańsk and at the Universitätsrechenzentrum of the Friedrich-Schiller University in Jena.

## References

1. Y. Nunes, G. Martins, N.J. Mason, D. Duflot, S.V. Hoffmann, J. Delwiche, M.-J. Hubin-Franskin, P. Limão-Vieira, *Phys. Chem. Chem. Phys.* **12**, (2010) 15734-15743
2. M.A. Śmiałek, M.-J. Hubin-Franskin, J. Delwiche, D. Duflot, N.J. Mason, S. Vrønning-Hoffmann, G.G.B. de Souza, A.M.F. Rodrigues, F.N. Rodrigues, P. Limão-Vieira, *Phys. Chem. Chem. Phys.* **14**, (2012) 2056-2064
3. K. Khistyayev, K.B. Bravaya, E. Kamarchik, O. Kostko, M. Ahmed, A.I. Krylov, *Faraday Discuss.* **150**, (2011) 313-330
4. K.B. Bravaya, O. Kostko, S. Dolgikh, A. Landau, M. Ahmed, A.I. Krylov, *J. Phys. Chem. A.* **114**, (2010) 12305-12317
5. M.P.S. Mateus, B.J.C. Cabral, *Chem. Phys. Lett.* **448**, (2007) 280-286
6. J.M. Riveros, E.B. Wilson, *J. Chem. Phys.* **46**, (1967) 4605-4612
7. Z. Peng, S. Shlykov, C. Van Alsenoy, H.J. Geise, B. Van der Veken, *J. Phys. Chem.* **99**, (1995) 10201-10212
8. M.A. Śmiałek, M.-J. Hubin-Franskin, J. Delwiche, M. Labuda, J. Guthmuller, D. Duflot, N.J. Mason, S. Vrønning-Hoffmann, N.C. Jones, P. Limão-Vieira: in preparation.
9. M. J. Frisch, G.W. Trucks, H.B. Schlegel, G.E. Scuseria, M.A. Robb et al.: GAUSSIAN 09, Inc., Wallingford CT. (2009).
10. A.D. Becke, *J. Chem. Phys.* **98**, (1993) 5648
11. C. Lee, W. Yang, R.G. Parr, *Phys. Rev. B.* **37**, (1988) 785
12. J.-D. Chai, M. Head-Gordon, *J. Chem. Phys.* **128**, (2008) 084106
13. A.D. Becke, *Phys. Rev. A.* **38**, (1988) 3098
14. H. Iikura, T. Tsuneda, T. Yanai, K. Hirao, *J. Chem. Phys.* **115**, (2001) 3540-3544
15. T. Schwabe, S. Grimme, *Phys. Chem. Chem. Phys.* **9**, (2007) 3397-3406
16. T.H. Dunning, *J. Chem. Phys.* **90**, (1989) 1007-1023
17. F. Duschinsky: *Acta Physicochim. URSS.* **7**, (1937) 551
18. T.E. Sharp, H.M. Rosenstock, *J. Chem. Phys.* **41**, (1964) 3453-3463
19. P.T. Ruhoff, *Chem. Phys.* **186**, (1994) 355-374
20. J. Guthmuller, F. Zutterman, B. Champagne, *J. Chem. Theory Comput.* **4**, (2008) 2094-2100
21. J. Guthmuller, F. Zutterman, B. Champagne, *J. Chem. Phys.* **131**, (2009) 154302
22. J. Guthmuller, B. Champagne, *ChemPhysChem.* **9**, (2008) 1667-1669
23. J. Guthmuller, B. Champagne, C. Moucheron, A. Kirsch - De Mesmaeker, *J. Phys. Chem. B.* **114**, (2010) 511-520
24. J.P. Merrick, D. Moran, L. Radom, *J. Phys. Chem. A.* **111**, (2007) 11683-11700